Calculation of the energy-averaged scattering function from high resolution low-energy neutron scattering data

C. H. Johnson and N. M. Larson
Oak Ridge National Laboratory, Oak Ridge, Tennessee 37830

C. Mahaux
Institut de Physique, Université de Liège, 4000 Liège, Belgium

R. R. Winters
Denison University, Granville, Ohio 43023
(Received 15 November 1982)

The elastic scattering neutron cross section at low energy displays many narrow resonances. By definition, the optical-model scattering function is equal to a suitable energy average of the actual scattering function. This average should be independent of the particular representation chosen for parametrizing the actual scattering function and also fairly independent of the averaging weight function. In particular, it should be fairly independent of the width of the weight function, even though a sparsity of resonances might require the width to be comparable to the energy range of the measurements. It is shown by direct numerical calculations of the average that this holds in the example of the scattering of $p_{3/2}$ neutrons by ^{32}S. Attention is drawn to pitfalls which exist when this average is evaluated analytically from parametrized forms of the scattering function. Several ways of graphically representing or of parametrizing the average scattering function are illustrated and discussed.

[NUCLEAR REACTIONS High resolution R-matrix scattering function, average scattering function, and optical model scattering function; application to $^{32}S+n$ for $p_{3/2}$ neutrons.]

I. INTRODUCTION

The optical model is one of the most useful tools of nuclear physics from the theoretical as well as from the practical point of view. For simplicity, we consider here the case in which only one channel is open for a given angular momentum and parity. The optical-model scattering function $S^{\mathrm{OM}}(E)$ at energy E is usually defined as being equal to the energy average $\langle S(E)\rangle_I$ of the scattering function $S(E)$:

$$S^{\mathrm{OM}}(E)=:\langle S(E)\rangle_I \ , \tag{1.1}$$

where I denotes the averaging interval. Experimentally for low energy nucleons, particularly for neutrons, the detailed energy dependence of the scattering function $S(E)$ for each significant partial wave can be determined from high resolution cross section measurements. It becomes important to correctly average these data for each partial wave in order to compare with optical model descriptions of the scattering. Such a comparison is meaningful only if the right-hand side of Eq. (1.1) can be defined in such a way that it is essentially independent of the averaging interval I, of the weighting function used in performing the averaging, and of the particular parametrization used for representing $S(E)$.

Brown[1] has argued that the Lorentzian averaging weight function is particularly convenient, and that one has then

$$\langle S(E)\rangle_I \approx S(E+iI) \ . \tag{1.2}$$

In order to calculate the right-hand side of Eq. (1.2), one needs an explicit algebraic form for $S(E)$. In practice, this is obtained by fitting the data over a limited energy region, usually in the framework of R-matrix theory. One of the primary purposes of this paper is to point out that conditions necessary to justify the contour integration leading to Eq. (1.2) are *not* usually satisfied in the convenient and commonly used R-matrix parametrization for $S(E)$ and that, relatedly, the quantity $S(E+iI)$ may be a sensitive function of the averaging interval I. We

 ©1983 The American Physical Society

demonstrate two alternative techniques (one numerical, one analytic) for averaging $S(E)$, both of which are justified mathematically and yield consistent results.

Our presentation scheme is the following: In Sec. II, we calculate $\langle S(E)\rangle_I$ numerically from the parametric form of $S(E)$ determined[2] in the specific experimental case of scattering $p_{3/2}$ neutrons by ^{32}S; we show that the energy-average $\langle S(E)\rangle_I$ is nearly independent of the choice of the averaging interval I and of the averaging weight function. Therefore, the corresponding optical-model potential indeed need not refer to any specific averaging procedure. Also in Sec. II we describe several ways of representing $\langle S(E)\rangle_I$ graphically and briefly discuss their relative merits. In Sec. III, we explain why the R-matrix parametrization for $S(E)$ is incompatible with a straightforward application of Eq. (1.2). We show nevertheless how a close approximation to $\langle S(E)\rangle_I$ can be obtained analytically using the R-matrix parametrization introduced in Ref. 2. In Sec. IV we point out that a generalization of Eq. (1.1) is necessary to include experimental cases where the resonances are so narrow or so widely spaced as to have little influence on the average of $S(E)$. Even with this refinement we find that a good approximation to $S^{\mathrm{OM}}(E)$ is obtained analytically using the same parametrization of the R matrix as in Sec. III. In Sec. V, we establish contact between $\langle S(E)\rangle_I$ on one hand, and the neutron strength function and the smoothed R function on the other hand. In so doing we find simple expressions for deducing an approximate $\langle S(E)\rangle_I$ from the preceding R-matrix parametrization of the data. Our main conclusions are summarized in Sec. VI.

II. NUMERICAL CALCULATION OF THE AVERAGE SCATTERING FUNCTION

A. The scattering function

For a spin zero target, the angle-integrated elastic scattering neutron cross section for one partial wave is given by

$$\sigma(E)=\pi k^{-2}g\,|\,1-S(E)\,|^2\,, \tag{2.1}$$

where g is the familiar spin-statistical factor, E is the bombarding energy, and k is the neutron wave number at energy E.

The quantity $S(E)$ is the scattering function for the relevant partial wave. It is a complex function; for real E, we write

$$S(E)=S_r(E)+iS_i(E)\,. \tag{2.2}$$

If only one channel is open at energy E, $S(E)$ has modulus unity for each angular momentum and parity,

$$S_r^{\,2}(E)+S_i^{\,2}(E)=1\,. \tag{2.3}$$

The cross section may therefore be expressed in terms of the real part of S as

$$\sigma(E)=2\pi k^{-2}g\,[1-S_r(E)]\,. \tag{2.4}$$

It would be incorrect to infer from Eq. (2.4) that the measurement of $\sigma(E)$ determines only the real part of $S(E)$. Indeed, Eq. (2.3) enables one to find the magnitude of $S_i(E)$ once $S_r(E)$ is known; the physical observables are independent of the sign of $S_i(E)$. On the other hand, the energy average cross section $\langle\sigma(E)\rangle_I$ determines only the average of the real part of the scattering function:

$$\langle\sigma(E)\rangle_I=2\pi k^{-2}g\,[1-\langle S_r(E)\rangle_I]\,. \tag{2.5}$$

When going from Eq. (2.4) to Eq. (2.5), we assumed that the factor k^{-2} need not be averaged over.

B. Definitions of the energy average

The experimental data cover only a finite energy domain, $[E_l,E_u]$, whose lower and upper ends we denote by E_l and E_u. Hence, a meaningful numerical calculation of the average of $S(E)$ should involve only the quantities $S(E')$ with $E_l<E'<E_u$. We write accordingly

$$\langle S(\bar{E})\rangle_I=\int_{E_l}^{E_u}F_I(E,E')S(E')dE'\,, \tag{2.6}$$

where $\bar{E}$ is given by

$$\bar{E}(E)_I=\int_{E_l}^{E_u}F_I(E,E')E'dE'\,, \tag{2.7}$$

and the normalization of the weight function is

$$\int_{E_l}^{E_u}F_I(E,E')dE'=1\,. \tag{2.8}$$

We shall always take the averaging weight function $F_I(E,E')$ to be an even function of $(E-E')$, although the function is distorted as E approaches the end points of $[E_l,E_u]$. Equation (2.7) defines $\bar{E}$ as the energy average of the energy E. At the center of the experimental domain, $\bar{E}$ is equal to E. The quantity $\bar{E}$ is introduced for the following reason, which will be discussed in detail in Sec. IV. The definition of the optical-model scattering function $S^{\mathrm{OM}}(E)$ should involve only the average of the strongly energy dependent part of $S(E)$ in the domain $[E_l,E_u]$, i.e., that part which arises from resonances within or close to the domain. The functional energy dependence of the slowly varying part of $S(E)$ should not be affected by the averaging. The introduction of the average energy $\bar{E}$ helps in

fulfilling this requirement, since the average of the linear function $\alpha+\beta E$ is given by $\alpha+\beta\bar{E}$.

Three typical choices for $F_I(E,E')$ are considered here:

$$F_I^L(E,E')=\frac{f_L}{(E-E')^2+I_L{}^2}\ , \tag{2.9}$$

$$F_I^G(E,E')=f_G e^{-(E-E')^2/I_G{}^2}\ , \tag{2.10}$$

and

$$F_I^B(E,E')=f_B\theta(I_B-|E-E'|)\ . \tag{2.11}$$

These correspond, respectively, to a Lorentzian, a Gaussian, and a box weight function. The coefficients f are determined by the normalization condition (2.8), and are implicitly functions of energy E.

The quantities I_L, I_G, and I_B characterize the size of the averaging interval I. Henceforth, we shall somewhat arbitrarily identify $2I$ with the full width at half maximum of the weighting function F. Then

$$I=I_L=I_B=(\ln 4)^{-1/2}I_G\ . \tag{2.12}$$

Figure 1(a) shows the dependence upon E' of functions F^L, F^G, and F^B for $E=550$ keV and $2I=600$ keV. The value $E=550$ keV corresponds to the middle of the domain [0, 1100 keV] covered by the experimental data[2,3] in the case $n+{}^{32}$S, which is discussed in detail below.

Figure 1(b) shows the Lorentzian weight function for $2I=400$, 600, and 800 keV. Figure 2 shows the

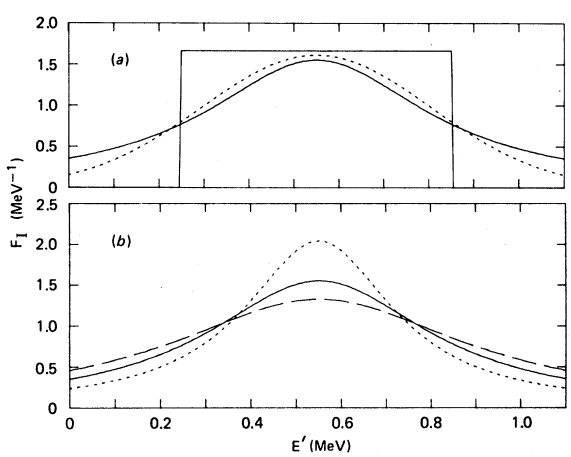

FIG. 1. Dependence upon E' of various weight functions $F_I(E,E')$ for $E=550$ keV, each normalized to unity in the interval [0, 1100 keV]. In (a) all curves have full width at half maximum $2I=600$ keV with the solid curve corresponding to the Lorentzian (2.9), the dots to the Gaussian (2.10), and the rectangle to the "box" (2.11). (b) shows the Lorentzian with $2I=400$ keV (dots), 600 keV (solid curve), and 800 keV (long dashes).

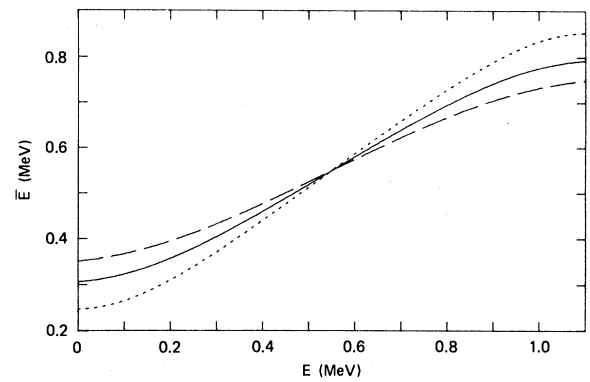

FIG. 2. Dependence upon the energy E of the average energy $\bar{E}$ as defined by Eq. (2.7), in the case of the Lorentzian weight function (2.9), with $2I=400$ keV (dots), 600 keV (full curve), and 800 keV (long dashes).

average energy $\bar{E}$, as defined in Eq. (2.7), vs E for the Lorentzian weight function and for these three values of the averaging interval I.

In the case of $p_{3/2}$ neutrons on ^{32}S, the average spacing D between neighboring resonances below 1100 keV is about 160 keV.[2,3] In order to obtain a meaningful average, the averaging energy interval I should satisfy the inequalities

$$D<I<(E_u-E_l)\ . \tag{2.13}$$

This is not an ideal situation. Ideally we would have the inequalities

$$D\ll I\ll(E_u-E_l)\ , \tag{2.14}$$

but often this is not encountered in light nuclei. In the case of $p_{3/2}$ neutrons on ^{32}S, inequalities (2.13) are satisfied for $I=300$ or 400 keV. The value $I=200$ keV is already somewhat too small since no $p_{3/2}$ resonances are observed between 412 and 714 keV, a region near the energy domain's center where the average $\langle S(E)\rangle_I$ is normally expected to be most unambiguously defined. This is precisely one of the reasons that the example $n+{}^{32}$S is instructive, since the problems encountered in that case are rather typical for light nuclei or for nuclei near closed shells.

C. Representations of the energy average

A straightforward way of representing $\langle S(E)\rangle_I$ would be to show its real and imaginary parts. However, it is more meaningful to present two quantities which are more directly related to the experimentally observed resonances and to the nonresonance background. One example of such a pair of quantities is the shape elastic and the compound nucleus cross sections,

$$\sigma_{se}(E)=\pi k^{-2}g\,|\,1-\langle S(E)\rangle_I\,|^2 \tag{2.15}$$

and

$$\sigma_c(E)=\pi k^{-2}g(1-|\,\langle S(E)\rangle_I\,|^2)\ . \tag{2.16}$$

Other representations of $\langle S(E)\rangle_I$ can be chosen which maintain the correlation to the experimental resonance and nonresonance cross sections. For instance, MacDonald *et al.*[4,5] proposed to write

$$\langle S(E)\rangle_I=\exp[2i\delta(E)]\ , \tag{2.17}$$

and to plot the real and imaginary parts of the optical model phase shift δ:

$$\delta(E)=\delta_r(E)+i\delta_i(E)\ . \tag{2.18}$$

The δ_r and δ_i are rather closely related to σ_{se} and σ_c, respectively.

Yet another representation is inspired by R-matrix theory[6,7] and consists of writing

$$\langle S(E)\rangle_I=e^{-2i\phi(E)}\frac{1+iP(E)[\bar{R}(E)+i\pi s(E)]}{1-iP(E)[\bar{R}(E)+i\pi s(E)]}\ , \tag{2.19}$$

where ϕ and P denote the hard sphere phase shift and penetrability, and where the real quantities $\bar{R}$ and s are the smoothed R function and the strength function, respectively. A disadvantage of this representation is that all these quantities depend upon the choice of the interaction radius a. One advantage is that the threshold behavior at $E\rightarrow 0$ is contained in the penetrability and not in $\bar{R}$ or s; $\bar{R}$ and s may then be parametrized by simple algebraic expressions such as contants or linear functions of E.

In contrast, the representations in terms of compound or shape-elastic cross sections and in terms of complex phase shifts do not depend on the choice of channel radius, but also do not factor out threshold behavior. For example, for s-wave neutrons we have

$$-\lim_{E\rightarrow 0}\frac{\delta_r(E)}{k}=R'\ , \tag{2.20}$$

where R' is the potential scattering length. The conventional s-wave strength function is given by

$$S_0=\frac{2k_0}{\pi}\lim_{E\rightarrow 0}\frac{\delta_i(E)}{k}\ , \tag{2.21}$$

where k_0 is evaluated at 1 eV. It thus appears that in the case of l-wave neutrons it might be more useful to plot the ratios $\delta_r(E)/k^{2l+1}$ and $\delta_i(E)/k^{2l+1}$ rather than $\delta_r(E)$ and $\delta_i(E)$.

D. Numerical results for $n+{}^{32}S$

In the present subsection, we calculate the average value of $S(E)$ in the case of the scattering of $p_{3/2}$ neutrons by ^{32}S in the experimental energy domain [0, 1100 keV]. The experimental data are described in Refs. 2 and 3. Resonances with $J^\pi=\frac{3}{2}^-$ have been observed at the energies $E_\lambda=97.5$, 112.2, 288.4, 412.3, 740.8, 778.6, 920.7, and 1091.4 keV. Our main purpose is to show that $\langle S(\bar{E})\rangle_I$ is well defined, i.e., is fairly independent of the averaging interval I and of the choice of the weight function $F(E,E')$. We consider the Lorentzian, Gaussian, and box averaging weight functions. The input is a parametric expression for $S(E)$ which is given in Ref. 2 and which is discussed in Sec. III. We emphasize that since the definition (2.6) of the average involves only "measured" values of $S(E)$, any other accurate parametrization of the data would lead to the same value for the average S function; this has been verified numerically.

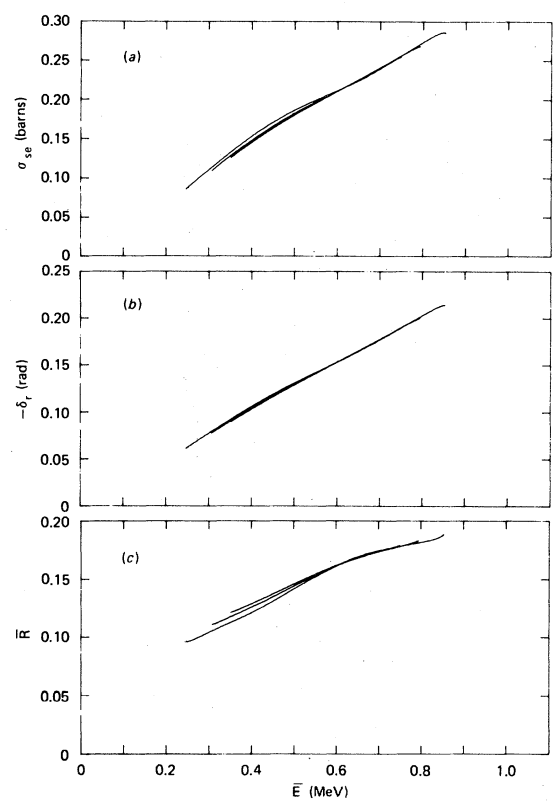

FIG. 3. Dependence upon the average energy of the three quantities which are closely related to the off resonance scattering in the case of $p_{3/2}$ neutrons on ^{32}S in the observed domain from 0 to 1.1 MeV. The quantities are (a) σ_{se} from Eq. (2.15), (b) δ_r from Eq. (2.18), and (c) $\bar{R}$ from Eq. (2.19) for a 6.4-fm channel radius. The Lorentzian weight function (2.10) has been used. Each figure shows curves for $2I=400$, 600, and 800 keV with that for 400 keV being the longest and that for 800 keV being the shortest curves.

1. *Lorentzian averaging weight function*

The related quantities σ_{se}, δ_r, and $\bar{R}$ defined by Eqs. (2.15), (2.18), and (2.19) are plotted in Figs. 3(a), (b), and (c), respectively, for the Lorentzian weight function (2.9) for $2I=400$, 600, and 800 keV. Since the plotted quantities depend mostly on the slowly varying off-resonance cross sections, they are each found to be practically independent of the averaging interval. Note that this would not be the case if we had not introduced the average energy $\bar{E}$ on the left-hand side of Eq. (2.6).

The related quantities σ_c, δ_i, and s are plotted in Figs. 4(a), (b), and (c), respectively, for the same weight functions as Fig. 3. Since these quantities are each closely related to the resonance structure they are more sensitive to the averaging interval. Near 550 keV for the narrowest Lorentzian, $2I=400$ keV, all three figures show a dip which reflects the absence of resonances between 412 and 740 keV; the larger values of $2I$, namely 600 and 800 keV, are thus more meaningful.

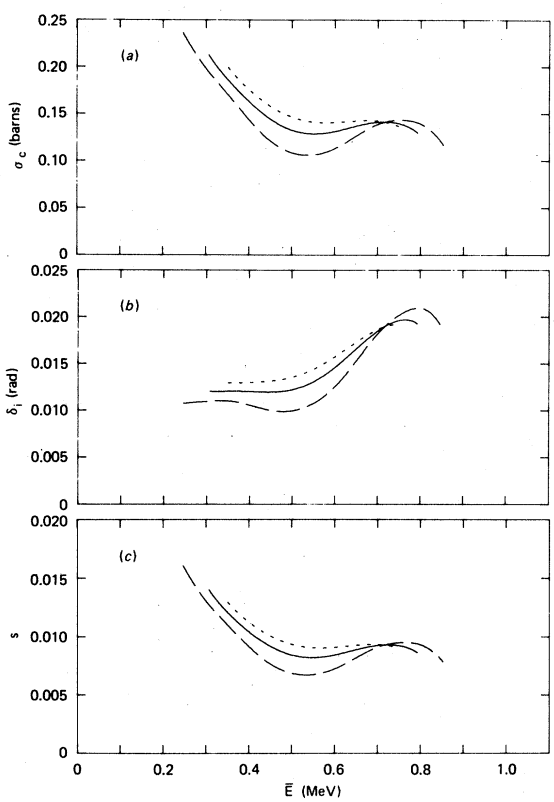

FIG. 4. Dependence upon the average energy of the three quantities which are closely related to the resonances observed in the case of $p_{3/2}$ neutrons on ^{32}S in the domain from 0 to 1.1 MeV. The quantities shown are (a) σ_c from Eq. (2.16), (b) δ_i from Eq. (2.18), and (c) s from Eq. (2.19) for a 6.4-fm channel radius. The Lorentzian weight function (2.9) has been used with $2I=400$ keV (dots), $2I=600$ keV (solid curve), and $2I=800$ keV (long dashes).

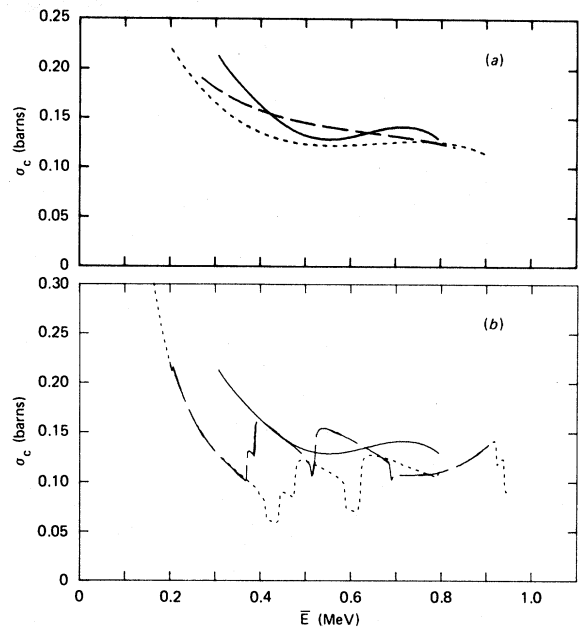

FIG. 5. Comparisons of the average compound cross section σ_c for various weight functions. In both (a) and (b) the full curve is reproduced from Figs. 4(a) for the Lorentzian for $2I=600$ keV. (a) includes the average for the Gaussian function, Eq. (2.10), for $2I=600$ keV (dots) and $2I=800$ keV (long dashes). (b) includes the box averages, Eq. (2.11), with the same dot and dash notation.

2. *Other weight functions*

We repeated the above calculations using the Gaussian and box weight functions. The resulting σ_{se}, δ_r, and $\bar{R}$ were not sensitive to the shape of the function; that was expected because they were insensitive to the width of the Lorentzian. However, since the quantities σ_c, δ_i, and s are sensitive to the width of the Lorentzian, we expect them also to be more sensitive to the choice of the function. In Figs. 5(a) and (b) we show σ_c for the Gaussian and the box weight functions, respectively. The box average does not lead to a smooth curve; abrupt changes occur each time an energy E_λ coincides with a sharp edge of the weighting function. But even in this case the results only fluctuate about the correct value of σ_c.

3. *Conclusion*

We conclude from Figs. 3–5 that the average scattering function can be quite well determined from the experimental data, even though in the

present case only a few resonances exist so that the averaging interval I cannot be chosen much larger than the level spacing D. In Sec. III, the average that we now have determined numerically will be compared with various analytical expressions which have been proposed in the literature. For that comparison we adopt as our "standard average" the evaluation of Eq. (2.6) with the Lorentzian weight function, Eq. (2.9), and with an averaging interval $I=300$ keV.

III. ANALYTICAL APPROXIMATIONS FOR THE AVERAGE SCATTERING FUNCTION

Since the integration of the scattering function cannot be done exactly in closed form, results obtained for $\langle S(\bar{E})\rangle_I$ from Eq. (2.6) are of necessity produced by numerical integration using carefully selected quadrature schemes. However, once a particular parametrization is chosen for the scattering function, it is possible to make approximations within the integrand and for the integration limits which yield an analytic form for the average scattering function. The analytic form thus obtained may be a good approximation to the standard average.

A. Parametrizations of the experimental data

A convenient way to analyze low energy neutron scattering data is based on the R-matrix formalism, which automatically embodies the unitary property (2.3). In the one-open-channel case, the scattering function is given by

$$S(E)=e^{-2i\phi(E)}\frac{1+iP(E)R(E)}{1-iP(E)R(E)}\ , \tag{3.1}$$

where the R function has the form

$$R(E)=\sum_{\mu=1}^{\infty}\frac{\gamma_\mu^{\ 2}}{E_\mu-E}\ . \tag{3.2}$$

The quantities E_μ and $\gamma_\mu^{\ 2}$ are real. In Eq. (3.1), we have chosen the boundary parameter B of R-matrix theory equal to the "shift function," whose energy dependence has for simplicity been neglected; this approximation becomes exact in the case of s-wave neutron scattering.

The fine structure data give information on the resonance energies E_μ only within the experimental domain, or at most slightly beyond the end points E_l and E_u of the domain. Let us denote by E_λ those observed resonance energies:

$$E_l<E_\lambda<E_u,\quad (\lambda=1,\ldots,N)\ . \tag{3.3}$$

The R function may then be written as

$$R(E)=R^{\text{int}}(E)+R^{\text{ext}}(E)\ , \tag{3.4}$$

where R^{int} is the "internal function" which contains the poles within $[E_l,E_u]$ and R^{ext} is the "external function" which contains the infinite series of poles outside the domain; thus

$$R^{\text{int}}(E)=\sum_{\lambda=1}^{N}\frac{\gamma_\lambda^{\ 2}}{E_\lambda-E} \tag{3.5}$$

and

$$R^{\text{ext}}(E)=\sum_{\mu>N}^{\infty}\frac{\gamma_\mu^{\ 2}}{E_\mu-E}\ . \tag{3.6}$$

In this form the analytic properties of $S(E)$, for complex E, are well understood; poles occur only in the lower half of the complex E plane. However, Eq. (3.6) for R^{ext} is not practical because the individual external poles are unknown; only their effects are measured within the experimental domain. From its definition R^{ext} must be a smoothly increasing function of energy within the domain. This function can be parametrized in any of several ways to give the correct $S(E)$, and any of these when introduced into Eq. (2.6) yields the correct standard average.

Often the experimental data are not sufficient to show the exact energy dependence of R^{ext}. For $p_{3/2}$ neutrons on ^{32}S the R^{ext} was deduced[2] from the resonance-background interference pattern at the eight resonance energies E_λ. Figure 6 shows the eight values with uncertainties. These data would permit a simple linear function for R^{ext}, but a better

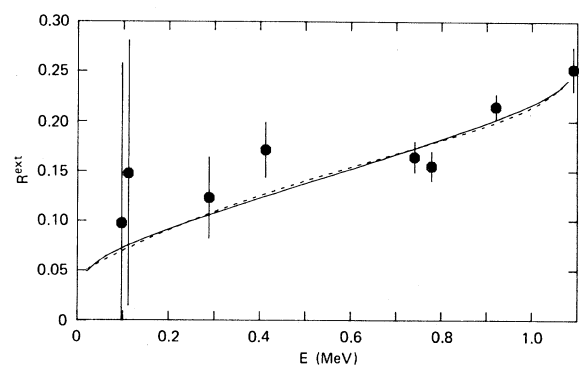

FIG. 6. Dependence upon energy of the external R function in the case of the scattering of $p_{3/2}$ neutrons by ^{32}S. The experimental points with associated uncertainties were obtained in Refs. 2 and 3 by fitting the resonance-background interference pattern at each of the eight resonances. The full curve was obtained by least squares adjustment to the data using a smoothed R function; see Eqs. (3.8)–(3.10). The dotted curve was obtained by adjusting the widths of a three-pole parametrization, Eqs. (3.11)–(3.13), to give a good fit to the full curve.

procedure is to adopt a function which approximates the shape expected from the definition (3.6). We shall consider the following two types of parametrization.

1. The empirical smoothed R function, $\tilde{R}$

Let us call $\tilde{s}$ the average value of the strength function $s(E)$ inside the experimental domain. From Fig. 4(c) and from the resonance parameters we see that $\tilde{s}$ is approximately equal to the ratio of the average width to the average spacing of the eight $p_{3/2}$ resonances,

$$\tilde{s} \simeq \langle \gamma^2 \rangle / D = 0.0093 \ . \tag{3.7}$$

Johnson and Winters[2] introduced the principal value integral

$$R^{\ln}(E) = \mathrm{P} \int_{E_l}^{E_u} \frac{\tilde{s}}{E'-E} dE' = \tilde{s} \ln \frac{E_u - E}{E - E_l} \ . \tag{3.8}$$

Following Lane and Thomas[6] they argued that, except near the end points where $R^{\ln}$ has singularities, the quantity

$$\tilde{R}(E) = R^{\mathrm{ext}}(E) + R^{\ln}(E) \tag{3.9}$$

is a smooth function of E which can usually be represented by a constant or by a linear function. The solid curve in Fig. 6 shows that, with $\tilde{s} = \langle \gamma^2 \rangle / D$, a good fit to R_{ext} is obtained with the linear form

$$\tilde{R}(E) = a + bE \ , \tag{3.10}$$

with $a = 0.083$ and $b = 0.113$ (MeV)$^{-1}$.

This parametrization ascribes the characteristic shape of $R^{\mathrm{ext}}(E)$ to the end point logarithmic singularities of $R^{\ln}(E)$. The physical origin of these singularities lies in the assumption that for an energy range of the order $E_u - E_l$ beyond the end points E_l and E_u, the external R function keeps approximately the same structure as the internal R function, i.e., has approximately the same strength function.

2. Few pole approximation for R^{ext}

Another parametrization of R^{ext} consists of expressing it as a sum of a few pole terms,

$$R^{\mathrm{ext}}(E) = \sum_{\alpha=1}^{M} \frac{\hat{\gamma}_\alpha^{\,2}}{\hat{E}_\alpha - E} \ . \tag{3.11}$$

Since R^{ext} must be a slowly varying smooth function within $[E_l, E_u]$, an adequate fit can be obtained with only a few poles, say four or less. The data in Fig. 6 could be described within the uncertainties by a single distant pole, but we have introduced three poles and adjusted the widths to give a good fit to the full curve for R^{ext} deduced above. The dashed curve in Fig. 6 shows the fit for

$$\hat{E}_\alpha = -1.0, 1.2, \text{ and } 11.2 \text{ MeV} \ , \tag{3.12}$$

and, respectively,

$$\hat{\gamma}_\alpha^{\,2} = 0.235, 0.0058, \text{ and } 3.10 \text{ MeV} \ . \tag{3.13}$$

Numerical calculations showed, as expected, that the standard average is essentially the same with this representation of R^{ext} as with the smoothed R-function parametrization.

The caret on the quantities $\hat{E}_\alpha$ and $\hat{\gamma}_\alpha^{\,2}$ is a reminder that these are merely parameters and should *not* be identified with the actual poles E_μ and reduced widths $\gamma_\mu^{\,2}$. Indeed, a drawback of the parametrization (3.11) is that it amounts to assuming that the structure of the R function, e.g., the pole spacing, is very different outside the domain $[E_l, E_u]$ from that inside. One is not allowed to attach any physical meaning to the right-hand side of Eq. (3.11) for values of E outside of the domain $[E_l, E_u]$.

B. Erroneous extensions into the complex plane

If the representation (3.1) is introduced into the averaging integral, Eq. (2.6) becomes

$$\langle S(\bar{E}) \rangle_I = \int_{E_l}^{E_u} e^{-2i\phi(E')} \frac{1 + iP(E')R(E')}{1 - iP(E')R(E')} \times F_I(E,E') dE' \ . \tag{3.14}$$

We now consider evaluating the integral by contour integration with the scattering function, or various approximations to it, extended into the complex plane. In this section we discuss improper extensions which yield incorrect averages. In Sec. III C we use a proper extension which yields a good approximation to our standard average.

1. $S(E+iI)$

Brown[1] proposed to approximate Eq. (3.14) by choosing the Lorentzian weight function, extending the limits to $\pm\infty$, closing the contour in the upper half of the complex energy plane, and evaluating the integral using the theorem of residues. Following this proposal, one usually writes

$$\langle S(E) \rangle_I = \int_{E_l}^{E_u} = \oint_{\mathrm{c.s.}} - \int_{-\infty}^{E_l} - \int_{E_u}^{\infty} - \oint_{\mathrm{o.s.}} \simeq \oint_{\mathrm{c.s.}} = S(E+iI) \ , \tag{3.15}$$

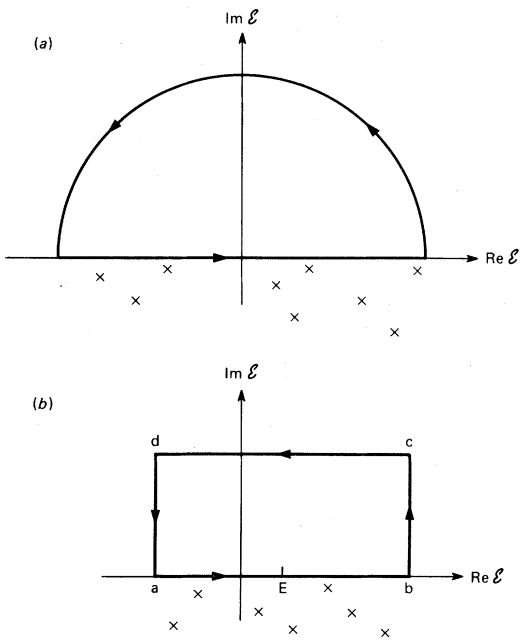

FIG. 7. Sketches of two integration contours used to argue that the average S matrix is related to $S(E+iI)$. The crosses represent poles of $S(\epsilon)$. (a) is a semicircular contour used for Eq. (1.2) or an extension thereof; see Eq. (3.15). (b) is a box contour used for Eq. (1.2) or an extension thereof; see Eq. (3.17). The distance ab is $2\alpha I$ and the distance bc is I.

where c.s. denotes a closed and o.s. an open semicircle and where the integrand has been suppressed for clarity. The closed contour is illustrated in Fig. 7(a). Since all such poles are in the lower half of the complex ϵ plane, one argues that the only contribution to the value of the integral is from the pole at $E+iI$ in the Lorentzian weight function.

However, the approximation indicated in Eq. (3.15) is invalid for any practical R-matrix parametrization because the integrand (and thus the integral) is not vanishingly small along the semicircle contour in the complex plane. To understand this, note that we may set $E'=\eta e^{i\theta}$ with $0<\theta<\pi$ and $\eta\to\infty$ to describe the semicircle. Then, for $\phi(E')=\beta(E')^{1/2}$ (where β is a positive constant), we find

$$e^{-2i\phi(E)}\to\frac{\exp[2\beta\sqrt{\eta}\sin\theta/2]}{\exp[2i\beta\sqrt{\eta}\cos\theta/2]}\ . \tag{3.16}$$

Since the exponent in the numerator is both real and positive for $0<\theta<\pi$, the integrand grows exponentially as the radius of the semicircle increases. The integral over the negative real axis is likewise nonnegligible, as can be seen by setting $\theta=\pi$ ($E'=-\eta$) in Eq. (3.16).

Direct comparisons of $S(E+iI)$ with our standard average support these criticisms. In Fig. 8, the

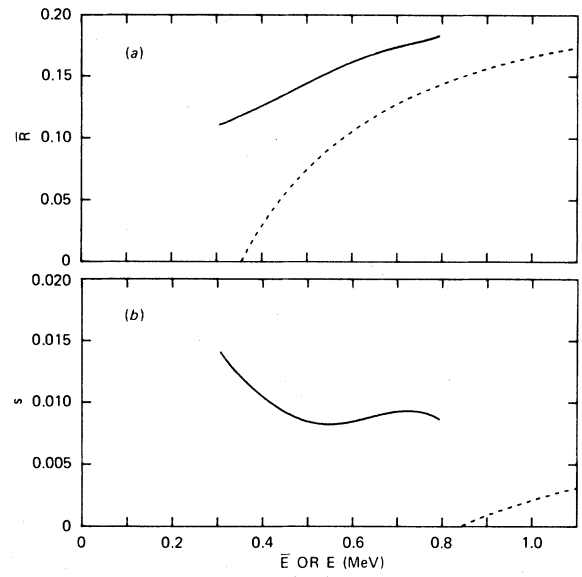

FIG. 8. A comparison for $2I=600$ keV of the "standard" values of $\bar{R}$ and s vs $\bar{E}$ [full curves reproduced from Figs. 3(c) and 4(c)] with those values (dotted curves) deduced from expressing $S(E+iI)$ in terms of $\bar{R}$ and s as in Eq. (2.19). The pole expansion of R^{ext} [see Eqs. (3.11)–(3.13) was used for $S(E+iI)$.

dotted curves represent the values of $\bar{R}$ and s [see Eq. (2.19)] obtained by replacing E by $E+iI$ in the scattering function S. The solid curves are the correct results obtained in Figs. 3(c) and 4(c) by the numerical averaging technique. Obviously the two sets of results are seriously discrepant. For calculating $S(E+iI)$ we used the three-pole representation of R^{ext}. Similar results were obtained using the empirical smoothed R-function representation.

A second method of approximating Eq. (3.14) is to use the box weight function, following a proposal by Lynn.[7] One then sets

$$\begin{aligned}\langle S(E)\rangle_I^B=\int_{E_l}^{E_u}&\simeq\int_{E-\alpha I}^{E+\alpha I}\\ &=\oint_{\substack{\text{c.b.}\\(a\to b\to c\to d\to a)}}-\oint_{\substack{\text{b.b.}\\(b\to c\to d\to a)}}\\ &\simeq S(E+iI)\ ,\end{aligned} \tag{3.17}$$

where c.b. denotes a closed and b.b. a bottomless box and where the closed contour is shown in Fig. 7(b) with the vertical distance, $ad=bc$, set equal to I. For $\alpha=\frac{1}{2}$ this is the form considered by Feshbach, Porter, and Weisskopf.[8] For $\alpha=1$ this form corresponds to our box average defined in Eqs. (2.6) and (2.11) provided $E_l+I<E<E_u-I$.

One then argues that, at a distance I above the real axis, $S(E+iI)$ is independent of E' within the domain $E-\alpha I<E'<E+\alpha I$, so that the integral

along the top of the box from c to d yields $-S(E+iI)$. Further, one assumes that the contributions from the vertical sides, bc and da, will cancel. Since integration along the entire closed contour yields zero, Eq. (3.17) follows.

That this result is incorrect we have seen above. Both the argument that $S(E+iI)$ is independent of E and the assumption that the vertical sides cancel are, in general, not justified.

2. $R(E+iI)$

Actually both Brown[1] and Lynn[7] used an approximation to the scattering function for their contour integrations, and the analytic extension of that approximation into the complex ϵ plane is far better behaved than the extension of the scattering function itself. They argued that, since the hard-sphere phase shift and the penetrability are slowly varying functions of energy within the experimental domain, a good approximation to Eq. (3.14) results from setting $E' \simeq \bar{E}$ in ϕ and P,

$$\langle S(\bar{E})\rangle_I \simeq e^{-2i\phi(\bar{E})} \int_{E_l}^{E_u} \frac{1+iP(\bar{E})R(E')}{1-iP(\bar{E})R(E')} \times F_I(E,E')dE' . \tag{3.18}$$

The remaining E' dependence of the integrand occurs in the R function and in the weight function.

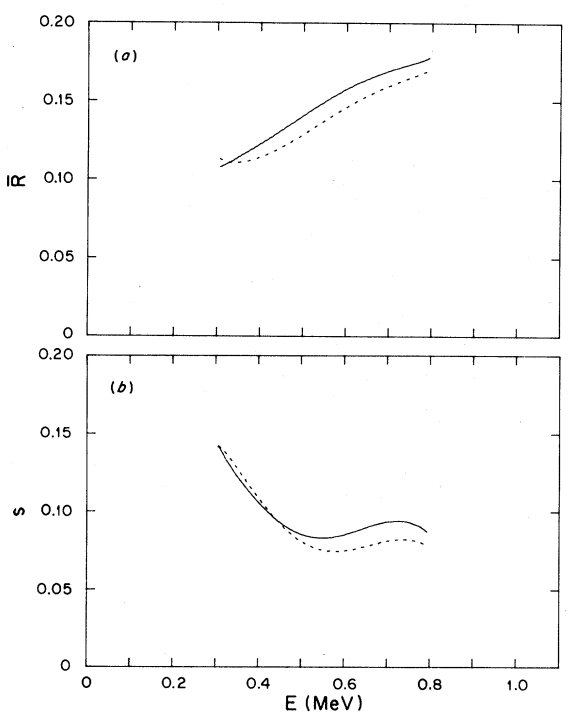

FIG. 9. A comparison for $2I=600$ keV of the standard values of $\bar{R}$ and s [full curves reproduced from Figs. 3(c) and 4(c)] with those values (dotted curves) obtained by approximating the hard-sphere phase shift and penetrability by $\phi(\bar{E})$ and $P(\bar{E})$ as in Eq. (3.18).

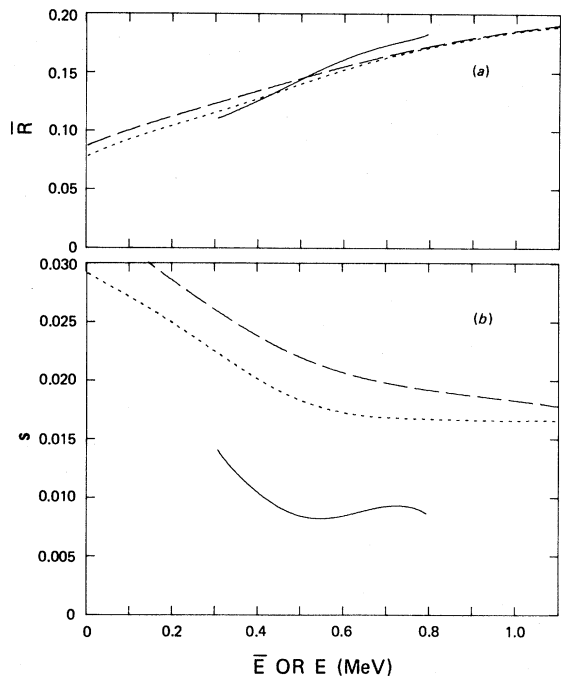

FIG. 10. A comparison as in Fig. 8 except that the dotted curves were deduced by evaluating $R(E+iI)$ in Eq. (3.19) and expressing the equation in the form of Eq. (2.19). The additional curves (long dashes) for $2I=800$ keV demonstrate the strong I dependence for s.

In order to examine this approximation we calculated the integral in Eq. (3.18) numerically and expressed it as $\bar{R}$ and s from Eq. (2.19) for comparison to our standard average. From Fig. 9, which shows $\bar{R}$ and s obtained by the two evaluations, we conclude that the approximation is quite acceptable in this case of $p_{3/2}$ neutrons on ^{32}S.

One might expect, therefore, that extension of the integrand of Eq. (3.18) into the complex plane would be straightforward because the difficulties reported in the previous subsection resulted primarily from the analytic extension of $\phi(E')$ and $P(E')$. Thus, we might expect that the expression

$$e^{-2i\phi(E)} \frac{1+iP(E)R(E+iI)}{1-iP(E)R(E+iI)} \tag{3.19}$$

would be a good approximation to the standard average. However, calculations using this expression show that it can be a bad approximation. Figure 10 compares the results of (3.19) for $I=300$ and 400 keV with the standard average, in the form of $\bar{R}$ and s from Eq. (2.19). We see that the strength function has a large discrepancy which increases with I. The same discrepancy occurs for both the few pole and the smoothed R-function representations of R^{ext}. In the latter case the strength $s(E)$ includes a term

bI/π, where b is the slope of the smoothed R function of Eq. (3.10). This spurious term gives rise to the large I dependence in Fig. 10.

Exactly where the underlying assumptions for the two contour integration methods are violated is more easily seen for the box weight. The requirement that the contributions from the two vertical sides cancel will be met only by accident, since it is unlikely that an arbitrary parametrization of $R(E')$ will have the property that R is the same along the two sides, i.e., that $R(E'=E-\alpha I+iy)$ is equal to $R(E'=E+\alpha I+iy)$ for $0\le y\le I$. Similarly, one could not expect that $R(E'+iI)$ is independent of E' for $E-\alpha I<E'<E+\alpha I$.

3. $R^{int}(E+iI)$

In the preceding prescriptions the calculated strength function $s(E)$ has a spurious component related to the behavior of $R^{\text{ext}}(E')$ for E' outside the domain $[E_l,E_u]$. Therefore, one might reasonably choose to replace E by $E+iI$ only in the internal R function, $R^{\text{int}}(E)$. Thus, one asks whether or not the expression

$$e^{-2i\phi(E)}\frac{1+iP(E)[R^{\text{ext}}(E)+R^{\text{int}}(E+iI)]}{1-iP(E)[R^{\text{ext}}(E)+R^{\text{int}}(E+iI)]} \quad (3.20)$$

is a good approximation to $\langle S(E)\rangle_I$. Let us write expression (3.20) in terms of $\bar{R}$ and s as in Eq. (2.19); this yields the approximation

$$\bar{R}(E)\approx R^{\text{ext}}(E)+\sum_{\lambda=1}^{N}\frac{(E_\lambda-E)\gamma_\lambda^2}{(E_\lambda-E)^2+I^2} \quad (3.21)$$

and

$$s(E)\approx\frac{I}{\pi}\sum_{\lambda=1}^{N}\frac{\gamma_\lambda^2}{(E_\lambda-E)^2+I^2}\ . \quad (3.22)$$

For large values of I as discussed above the right-hand side of Eq. (3.22) decreases with increasing I, whereas the physical strength function should be independent of I. Hence, expression (3.20) is also not an accurate representation of $\langle S(E)\rangle_I$, except in the idealized case where inequalities $D\ll I\ll(E_u-E_l)$ are fulfilled. Then, indeed, the right-hand side of Eq. (3.22) can be replaced by $\langle\gamma^2\rangle/D$. For light nuclei, however, the interval I often cannot be taken much smaller than E_u-E_l, since it must be larger than D. Again, the unphysical results arise from the non-negligible contributions for energies E' outside the domain $[E_l,E_u]$ either $E'<E_l$, $E'>E_u$, or the vertical sides for the box average.

C. The uniform R function

Having demonstrated that several contour integrations are improper, we now show that it is possible to express the R function as the sum of two terms, the first of which is slowly varying such that it may be fixed at $E'=E$ and the second of which is a uniform R function which satisfies the requirements of the contour integration.

1. Theoretical development

Following Lane and Thomas,[6] we define the uniform R function to include the observed poles of the domain plus a sum of outer poles which have the same statistical properties as those inside,

$$R^{\text{uni}}(E')=R^{\text{int}}(E')+\sum_\alpha\frac{\hat{\gamma}_\alpha^2}{\hat{E}_\alpha-E'}\ , \quad (3.23)$$

where $R^{\text{int}}(E')$ is given by Eq. (3.5), and the summation involves only values of $\hat{E}_\alpha$ outside of $[E_l,E_u]$. The caret notation is used here, just as in the few-pole representation of Eq. (3.11), to emphasize that the poles are not the actual ones outside of the domain. The exact values of $\hat{\gamma}_\alpha^2$ and $\hat{E}_\alpha$ cannot be specified, since only their statistical properties (i.e., the pole strength and pole density) are assumed. Even the statistical properties are not necessarily representative of the region just outside of the domain.

We wish to evaluate (3.23) for E' within the domain. Since the E_α are outside, only the tails of these poles contribute. Therefore the summation may be approximated by an integral over the outer region,

$$R^{\text{uni}}(E')\simeq R^{\text{int}}(E')+\int_{-\infty}^{E_l}\frac{s(E'')dE''}{E''-E'}+\int_{E_u}^{\infty}\frac{s(E'')dE''}{E''-E'}\ , \quad (3.24)$$

where $s(E'')$ is the same strength function as that associated with $R^{\text{int}}(E')$ for E' near E. That is, $s(E'')$ may be approximated by $\tilde{s}(E)$. Therefore, for E' near E, the uniform R function becomes

$$R_E^{\text{uni}}(E')\simeq R^{\text{int}}(E')-\tilde{s}(E)\int_{E_l}^{E_u}\frac{dE''}{E''-E'}+\tilde{s}(E)\int_{-\infty}^{\infty}\frac{dE''}{E''-E'}\ . \quad (3.25)$$

The integral with infinite limits vanishes, and the uniform R function is seen to be of the form

$$R_E^{\text{uni}}(E')\simeq R^{\text{int}}(E')-\tilde{s}(E)\ln\frac{E_u-E'}{E'-E_l}\ . \quad (3.26)$$

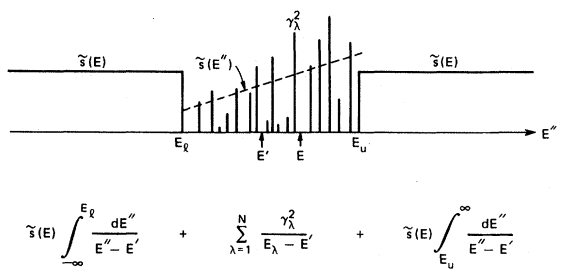

FIG. 11. Pictorial representation of the uniform R function. For E' near E this function is the sum of the two integrals over the outer region plus the summation over the inner region. See Eqs. (3.24)–(3.26). Here the average strength function $\tilde{s}(E'')$ is shown to be linearly increasing from E_l to E_u.

The preceding definition of R_{uni} is shown pictorially in Fig. 11.

The remainder of the R function, i.e., the slowly varying part for E' near E, is found by subtraction,

$$\tilde{R}(E')=R(E')-R_E^{\text{uni}}(E') \ . \tag{3.27}$$

Substituting from Eqs. (3.4) and (3.26), we find

$$\tilde{R}(E')\simeq R^{\text{ext}}(E')+\tilde{s}(E)\ln\frac{E_u-E'}{E'-E_l} \ . \tag{3.28}$$

Since $\tilde{R}(E')$ is slowly varying, except near E_l and E_u, it may be approximated within the integrand of Eq. (3.18) by fixing its values at $E'=\bar{E}$ in the same manner that the hard-sphere phase shift and penetrability were fixed at $\bar{E}$. This gives the approximate average S function as

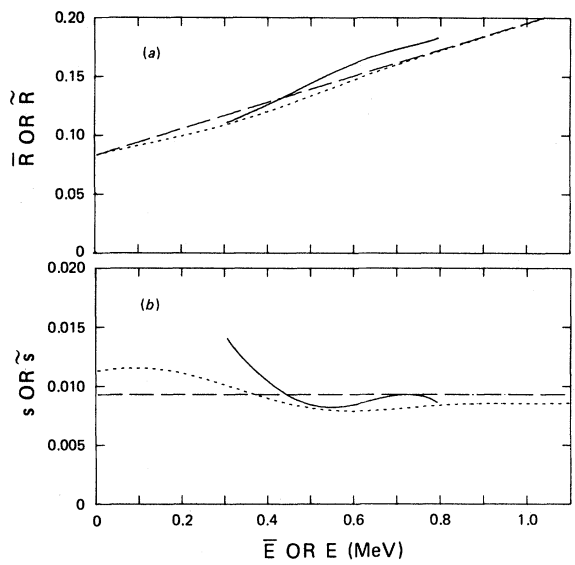

FIG. 12. A comparison for $2I=600$ keV of the standard values of $\bar{R}$ and s vs $\bar{E}$ [full curves reproduced from Figs. 3(c) and 4(c)] with those values versus E (dotted curves) deduced using the uniform R function, i.e., Eq. (3.30) expressed as Eq. (2.19). The dashed curves show only the leading terms, $\tilde{R}$ and $\tilde{s}$, in Eqs. (5.3) and (5.4).

$$\langle S(\bar{E})\rangle_I\simeq e^{-2i\phi(\bar{E})}\int_{E_l}^{E_u}\frac{1+iP(\bar{E})[\tilde{R}(\bar{E})+R_E^{\text{uni}}(E')]}{1-iP(\bar{E})[\tilde{R}(\bar{E})+R_E^{\text{uni}}(E')]}F_I(E,E')dE' \ . \tag{3.29}$$

Because $R_E^{\text{uni}}(E')$ is a uniform R function,[6] the requirements for the contour integration schemes are now met. Again we consider the box weight function; the contributions from the vertical sides, da and bc, do cancel here since the only E' dependence in the integrand of (3.29) is in the uniform R function. Also, the value of $R_E^{\text{uni}}(E')$ along the top of the box (i.e., at $E'\rightarrow E'+iI$) is independent of E', so $R_E^{\text{uni}}(E')$ may be set at $R^{\text{uni}}(E+iI)$ there. Thus we have the algebraic prescription

$$\langle S(E)\rangle_I\simeq e^{-2i\phi(E)}\frac{1+iP(E)[\tilde{R}(E)+R_E^{\text{uni}}(E+iI)]}{1-iP(E)[\tilde{R}(E)+R_E^{\text{uni}}(E+iI)]} \ . \tag{3.30}$$

2. *Use of R^{uni} and comparison to the numerical average*

To use Eq. (3.30) for averaging high resolution cross section data we first estimate $\tilde{s}$ from the widths and spacings of the resonances. For ^{32}S, $\tilde{s}$ can be approximated by the constant $\langle\gamma^2/D\rangle$, as in Eq. (3.7). (Justification for this approximation is given in Sec. V.) Given $\tilde{s}$ and the resonance parameters we calculate R_E^{uni} at $E+iI$ from Eq. (3.26); and given $\tilde{s}$ and the experimental R^{ext}, we calculate $\tilde{R}$ from Eq. (3.28). Since $\tilde{R}$ is a slowly varying function of energy it can be parametrized as a linear function as in Eq. (3.10). Such a parametrization is permitted because $\tilde{R}$ is needed only on the real axis.

Figure 12 shows the resulting $\langle S(E)\rangle_I$ from Eq. (3.30), expressed in terms of $\bar{R}$ and s from Eq. (2.19). By comparison with our standard average, which is reproduced from Figs. 3(c) and 4(c), we see that the contour integration using R^{uni} is a good approximation.

IV. THE OPTICAL-MODEL SCATTERING FUNCTION

In Sec. II, we demonstrated numerically that in the case of the scattering of $p_{3/2}$ neutrons by ^{32}S the right-hand side of Eq. (1.1) is approximately independent of the averaging interval I and of the averaging weight function $F(E,E')$. These properties are requested if one wants to use Eq. (1.1) for defining the optical-model scattering function $S^{\rm OM}(E)$. Generally, these properties do hold; however, there are some experimental cases where they do not hold because, as discussed in detail below, the resonances are too narrow or too widely spaced to significantly influence the average of $S(E)$. Hence, a refinement to the definition of Eq. (1.1) is necessary.

We first note that it is in the spirit of the optical model to average the variations of $S(E)$ about a smooth background. The arguments contained above, as well as for instance in Refs. 2 and 6, indicate that this background can be identified with the quantity

$$S_{\rm bgr}(E)=e^{-2i\phi(E)}\frac{1+iP(E)\widetilde{R}(E)}{1-iP(E)\widetilde{R}(E)}\ , \tag{4.1}$$

which has modulus unity. With this definition we have

$$S(E)=S_{\rm bgr}(E)\cdot S_{\rm res}(E)\ , \tag{4.2}$$

where the unitary function $S_{\rm res}(E)$ contains the energy dependence associated with the resonances inside or slightly outside the domain $[E_l,E_u]$. We now argue that it is more appropriate to define the optical-model scattering function by the equation

$$S^{\rm OM}(E)=S_{\rm bgr}(E)\cdot\langle S_{\rm res}(E)\rangle_I\ . \tag{4.3}$$

This equation includes Eq. (1.1) as the limiting case reached when the background is independent of energy.

To understand the need for these equations for the case of narrow widely spaced levels, let us consider the instructive limit $\widetilde{s}(E)\to 0$. Then, $S(E)$ reduces to the background (4.1). Unless the latter is exactly independent of energy, it differs from its energy average $\langle S_{\rm bgr}(E)\rangle_I$. The latter has modulus smaller than unity. One can thus write $\langle S_{\rm bgr}(E)\rangle_I$ in the form of Eq. (2.19), namely

$$\langle S_{\rm bgr}(E)\rangle_I=e^{-2i\phi(E)}\frac{1+iP(E)[\overline{R}_{\rm bgr}(E)+i\pi s_{\rm bgr}(E)]}{1-iP(E)[\overline{R}_{\rm bgr}(E)+i\pi s_{\rm bgr}(E)]} \tag{4.4}$$

The right-hand side of Eq. (4.4) contains a positive quantity $s_{\rm bgr}(E)$ which has no relationship whatsoever with the experimental strength function $\widetilde{s}=\langle\gamma^2\rangle/D$. It is thus clear that by averaging the full $S(E)$ one includes in the quantity $s(E)$ of Eq. (2.19) a contribution which arises from the energy dependence of the background. When $\langle\gamma^2\rangle/D$ is particularly small, this spurious contribution may even dominate the value of $s(E)$. This is the case for the scattering[9] of p-wave neutrons by ^{40}Ca, for which $\langle\gamma^2\rangle/D$ is one order of magnitude smaller than in the case of $p_{3/2}$ neutrons on ^{32}S.

The spurious contribution $s_{\rm bgr}(E)$ moreover increases with the averaging interval I. Indeed, the unitary function $S_{\rm bgr}(E)$ is represented by a point which moves along a portion of the unit circle as E increases from E_l to E_u; the average $\langle S_{\rm bgr}(E)\rangle_I$ is represented by a point which lies inside the unit circle, at a distance from it which is proportional to I, provided that I is small and that the energy dependence of $S_{\rm bgr}(E)$ is sufficiently smooth.

The occurrence of the spurious background contribution to the strength function can be avoided by defining the optical-model scattering function by Eq. (4.3). The reasoning carried out in Sec. III C 1 shows that in practice this amounts to the following simple prescription:

$$S^{\rm OM}(E)\simeq e^{-2i\phi(E)}\frac{1+iP(E)[\widetilde{R}(E)+R_E^{\rm uni}(E+iI)]}{1-iP(E)[\widetilde{R}(E)+R_E^{\rm uni}(E+iI)]}\ , \tag{4.5}$$

where $R_E^{\rm uni}(E')$ is defined by Eq. (3.26). The strength function $s(E)$ and the smoothed function $\overline{R}(E)$ can then be defined by the relation

$$S^{\rm OM}(E)=e^{-2i\phi(E)}\frac{1+iP(E)[\overline{R}(E)+i\pi s(E)]}{1-iP(E)[\overline{R}(E)+i\pi s(E)]}\ . \tag{4.6}$$

In the case of $p_{3/2}$ neutrons on ^{32}S, the results contained in Fig. 9 show that the definition (4.3) is approximately equivalent to (1.1). However, it will be shown elsewhere[10] that this is not the case for the scattering of p-wave neutrons by ^{40}Ca. In that case, indeed, the right-hand side of Eq. (1.1) depends upon I because of the occurrence of a spurious background contribution $s_{\rm bgr}(E)$ which is comparable to the actual strength function $s(E)$. The definition (4.3) rather than (1.1) must be used. This is a further illustration of the usefulness of the data analysis described in Sec. III C.

We emphasize that the quantities $S_{\rm bgr}(E)$, $S_{\rm res}(E)$, and the right-hand side of Eq. (4.5) are essentially independent of the parametrization of the fine structure data. Indeed, the background is experimentally well defined and the use of $\widetilde{R}$ instead of $R^{\rm ext}$ in Eq. (4.1) in effect amounts to defining a background

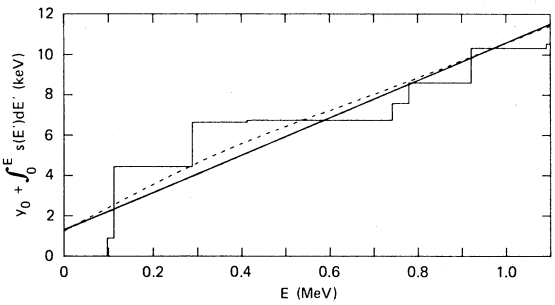

FIG. 13. Cumulative plot of the $p_{3/2}$ neutron reduced widths. The staircase is the experimental sum for the eight observed resonances. The straight solid line is the integral for constant $\tilde{s}=0.0093$ with the intercept y_0 adjusted for best fit to the staircase. For the dotted curve, $s(E)$ is from the dotted curve in Fig. 12(b), i.e., the result from using the uniform R function with $2I=600$ keV.

which is nearly independent of the precise location of the boundaries E_l and E_u of the experimental domain.

V. DATA ANALYSIS USING $\tilde{R}$ and R^{uni}

From high resolution neutron cross section data and the corresponding R-matrix parameters one can obtain an experimental $S^{\text{OM}}(E)$ by averaging for each partial wave as indicated by the right-hand side of Eq. (4.3). One can then describe this average by a model, say a phenomenological model with appropriate real and imaginary well depths. The averaging could be done numerically as in Sec. II; however, a good approximation is obtained more easily by contour integration using R^{uni} in Eq. (4.5). For this purpose the R^{ext} is parametrized in terms of a smoothed R-function, $\tilde{R}(E)$, as outlined in Sec. III A 1. In the example for $p_{3/2}$ neutrons on ^{32}S, the data are described adequately by a constant $\tilde{s}$ and linear $\tilde{R}(E)$; however, the $\tilde{s}$ in Eq. (3.8) could be an energy-dependent quantity, $\tilde{s}(E)$, and the $\tilde{R}(E)$ in Eq. (3.10) could be higher order than linear.

For constant $\tilde{s}$ an even simpler calculation can be made to give a good approximation to the contour integration. In fact, part of this simple calculation is a familiar procedure in the literature of neutron physics. In the following we show the connection to that procedure.

By expressing the approximation of Eq. (4.5) in the form of Eq. (2.19) we find

$$\bar{R}(E)=\tilde{R}(E)+\text{Re}R_E^{\text{uni}}(E+iI) \tag{5.1}$$

and

$$s(E)=\frac{1}{\pi}\text{Im}R_E^{\text{uni}}(E+iI)\ . \tag{5.2}$$

These equations can be rewritten in the form

$$s(E)=\tilde{s}(E)+s^f(E)\ , \tag{5.3}$$

and

$$\bar{R}(E)=\tilde{R}(E)+R^f(E)\ , \tag{5.4}$$

where the "fluctuating" s^f and R^f are given by

$$s^f(E)=\frac{I}{\pi}\sum_{\lambda=1}^{N}\frac{\gamma_\lambda^2}{(E_\lambda-E)^2+I^2} -\tilde{s}(E)\frac{I}{\pi}\int_{E_l}^{E_u}\frac{dE'}{(E'-E)^2+I^2} \tag{5.5}$$

and

$$R^f(E)=\sum_{\lambda=1}^{N}\frac{\gamma_\lambda^2(E_\lambda-E)}{(E_\lambda-E)^2+I^2} -\tilde{s}(E)\int_{E_l}^{E_u}\frac{(E'-E)dE'}{(E'-E)^2+I^2}\ . \tag{5.6}$$

If $\tilde{s}(E)$ can be approximated by the constant $\langle\gamma^2\rangle/D$, it is clear from Eqs. (5.5) and (5.6) that s^f and R^f are energy dependent but fluctuate about zero. Thus, to a good approximation

$$\bar{R}(E)\simeq\tilde{R}(E) \tag{5.7}$$

and

$$s(E)\simeq\langle\gamma^2\rangle/D\ . \tag{5.8}$$

In Fig. 12 the dashed curves show $\tilde{R}$ and $\langle\gamma^2\rangle/D$ for the case of $p_{3/2}$ neutrons on ^{32}S; indeed these are good approximations to $\bar{R}(E)$ and $s(E)$. This verifies that $\langle\gamma^2\rangle/D$ is a good estimate of $\tilde{s}$ for the contour integration.

The familiar procedure in the analysis of low-energy neutron scattering data is to identify the strength function with the slope of the straight line which best fits the staircase obtained by plotting versus E the quantity

$$\sum_{E_\lambda<E}\gamma_\lambda^2\ . \tag{5.9}$$

For ^{32}S $p_{3/2}$ waves this cumulative plot is shown in Fig. 13; it is to be compared with the straight line

$$y_0+\tilde{s}E\ , \tag{5.10}$$

where $\tilde{s}$ is set equal to $\langle\gamma^2\rangle/D$ and y_0 is a best fit intercept at $E=0$. Also shown in the figure is

$$y_0+\int_0^E s(E')dE' \tag{5.11}$$

where the function $s(E')$ is from the complete contour integration as shown in Fig. 12.

In the literature of neutron physics the strength

function s has usually been approximated from the staircase plot of the resonance data, but the corresponding evaluation of $\bar{R}$ from R^{ext} has often been omitted. (An exception occurs for very low energy s-wave neutrons where the familiar potential scattering radius R' is proportional to $1-\bar{R}$). But the evaluation of $\bar{R}$ and s are of equal importance for deducing an optical model potential; $\bar{R}$ and s are closely related, respectively, to the depths, V_0 and W_D, of the real and imaginary potentials. To illustrate the importance of the quantity $\bar{R}$ we cite the analysis of the ^{32}S data by Johnson and Winters.[2] They found the fitting of $\bar{R}$ with a phenomenological spherical optical model potential required a much deeper real well for p waves than for s waves. Subsequently MacKellar and Castel[11] showed that this l dependence could be removed by including deformation effects in the ^{32}S target.

IV. SUMMARY

By comparison with numerical averages, we have shown that the algebraic prescriptions most often encountered in the literature for calculating the average S function may lead to inaccurate results. The origin of these disagreements has been exhibited. We have argued on physical and analytical grounds and demonstrated numerically that replacing E by $E+iI$ only on the uniform part of the R function [see Eqs. (3.26), (3.28), and (3.30)] gives an accurate prescription for calculating the average S function. This average is approximately the optical model S function as indicated in Eq. (4.5).

In these equations, the average strength function $\tilde{s}(E)$ is the ratio $\langle\gamma^2\rangle/D$, i.e., the ratio of the observed average reduced width to the average spacing in the vicinity of the energy E; and the smoothed R function $\tilde{R}$ is determined by fitting the experimental external R function R^{ext} with the procedure used in Ref. 2 and described in Sec. III A 1. In fact, except for minor fluctuations, the $\tilde{R}(E)$ and $\tilde{s}(E)$ so derived are good approximations to the more detailed $\bar{R}(E)$ and $s(E)$ from Eqs. (3.30) and (2.19). Thus one is justified to use simply $\tilde{R}(E)$ and $\tilde{s}(E)$ in Eq. (4.6) for finding an average $S^{\text{OM}}(E)$ which can be compared to an optical model. Clearly, in such an analysis of experimental data, one must obtain both the strength function $\tilde{s}$ and the smoothed R function $\tilde{R}$.

ACKNOWLEDGMENTS

The present work was stimulated by lively discussions with Dr. W. M. MacDonald. We are also indebted to Dr. J. A. Harvey and Dr. G. R. Satchler for helpful discussions and for critical reading of this manuscript. C. Mahaux thanks the Oak Ridge National Laboratory for sponsoring the visit to Oak Ridge National Laboratory (ORNL), which made this collaboration possible. The research was sponsored by the Division of Nuclear Sciences, U.S. Department of Energy, under Contract Nos. W-7405-eng-26 with the Union Carbide Corporation and DE-AC02-76-ER02696 with Denison University.

[1] G. E. Brown, Rev. Mod. Phys. 31, 893 (1959).

[2] C. H. Johnson and R. R. Winters, Phys. Rev. C 21, 2190 (1980); Phys. Rev. C 27, 416 (1983). In Fig. 2 on p. 417 of this reference the ordinate labels should be 0.5, 1.0, and 1.5 rather than 1, 2, and 3.

[3] J. Halperin, C. H. Johnson, R. R. Winters, and R. L. Macklin, Phys. Rev. C 21, 545 (1980).

[4] W. M. MacDonald, C. H. Johnson, and R. R. Winters, Bull. Am. Phys. Soc. 26, 1139 (1981); 26, 1140 (1981).

[5] More recently W. M. MacDonald and M. C. Birse, University of Maryland Report ORO 5126-171, 1982 (unpublished), proposed that the complex phase shifts derived using $S(E+iI)$ be equated to the phase shifts calculated from an optical model at the same complex energy.

[6] A. M. Lane and R. G. Thomas, Rev. Mod. Phys. 30, 257 (1958).

[7] J. E. Lynn, *The Theory of Neutron Resonance Reactions* (Clarendon, Oxford, 1968).

[8] H. Feshbach, C. E. Porter, and V. F. Weisskopf, Phys. Rev. 71, 448 (1954).

[9] J. L. Fowler, C. H. Johnson, and N. W. Hill (unpublished).

[10] R. R. Winters, C. H. Johnson, and N. M. Larson (unpublished).

[11] A. D. MacKellar and B. Castel, Bull. Am. Phys. Soc. 27, 722 (1982).